

## Europium(III) DOTA-Derivatives Having Ketone Donor Pendant Arms Display Dramatically Slower Water Exchange

Kayla N. Green, Subha Viswanathan, Federico A. Rojas-Quijano, Zoltan Kovacs, and A. Dean Sherry\*

*Advanced Imaging Research Center, UT Southwestern Medical Center, 5323 Harry Hines Boulevard, Dallas, Texas 75390, United States and Department of Chemistry, University of Texas at Dallas, 800 West Campbell Road, Richardson, Texas 75080, United States*

Received September 9, 2010

A series of new 1,4,7,10-tetraazacyclododecane-derivatives having a combination of amide and ketone donor groups as side-arms were prepared, and their complexes with europium(III) studied in detail by high resolution NMR spectroscopy. The chemical shift of the  $\text{Eu}^{3+}$ -bound water resonance, the chemical exchange saturation transfer (CEST) characteristics of the complexes, and the bound water residence lifetimes ( $\tau_m$ ) were found to vary dramatically with the chemical structure of the side-arms. Substitution of ketone oxygen donor atoms for amide oxygen donor atoms resulted in an increase in residence water lifetimes ( $\tau_m$ ) and a decrease in chemical shift of the  $\text{Eu}^{3+}$ -bound water molecule ( $\Delta\omega$ ). These experimental results along with density functional theory (DFT) calculations demonstrate that introduction of weakly donating oxygen atoms in these complexes results in a much weaker ligand field, more positive charge on the  $\text{Eu}^{3+}$  ion, and an increased water residence lifetime as expected for a dissociative mechanism. These results provide new insights into the design of paramagnetic CEST agents with even slower water exchange kinetics that will make them more efficient for in vivo imaging applications.

### Introduction

Paramagnetic lanthanide compounds have had a substantial impact in NMR and magnetic resonance imaging (MRI) since the early 1970s. Gadolinium( $\text{Gd}^{3+}$ )-based  $T_1$  agents have served as the gold standard for MRI contrast agents since the late 1980s, and new directions for  $\text{Gd}^{3+}$  contrast agents continue to be an active area of research.<sup>1–4</sup> A variety of molecular designs have been reported as “responsive”  $\text{Gd}^{3+}$  contrast agents,<sup>5</sup> most based on changes in relaxivity that reflect either a change in  $q$  (number of inner-sphere water molecules) or  $\tau_R$  (molecular rotation). Although it has proven relatively easy to detect changes in  $T_1$  relaxation in response to biological events in vitro, it is more problematical in vivo because these complexes are never completely “silent” even if water has no direct access to the  $\text{Gd}^{3+}$  coordination sphere. This makes it problematic to distinguish between a change in relaxivity versus a change in concentration. Consequently, other approaches for introducing contrast in MR images are

being explored. One relatively promising technique is based on chemical exchange saturation transfer (CEST) principles.<sup>6</sup> This technique relies on the selective saturation of a small pool (A) of protons that are in exchange with the much larger bulk water pool (B). Exchange of saturated spins from pool A into B results in a decrease in the intensity of the bulk water spins because they become partially saturated as a result of the exchange. CEST requires slow-to-intermediate exchange between the two pools so by definition this depends upon the frequency difference between the two proton pools,  $\Delta\omega$ . Slow-to-intermediate exchange requires the condition,  $\Delta\omega\tau_m > 1$ , where  $\tau_m$  is the metal bound water residence lifetime. Large  $\Delta\omega$  values are advantageous for two reasons; first, a large  $\Delta\omega$  makes it easier to selectively saturate at one site without inadvertently partially saturating the other, and a large  $\Delta\omega$  allows faster exchanging systems to be used for CEST while maintaining the slow-to-intermediate requirement. The effectiveness of CEST agents is also dependent on the number of exchangeable sites ( $N$ ) contained within the CEST agent. The value of  $N$  is directly related to the sensitivity of the agent while  $\tau_m$  is a measure of the efficiency of exchange between the pools. Diamagnetic CEST agents such as barbituric acid, peptides, or nucleic acids have relatively small  $\Delta\omega$  values, typically  $< 5$  ppm, so proton exchange must be quite slow to meet the CEST requirement.<sup>7</sup> Complexes of paramagnetic

\*To whom correspondence should be addressed. Phone: +1 214-645-2755. Fax: +1 214-645-2744. E-mail: dean.sherry@utsouthwestern.edu.

(1) Caravan, P.; Ellison, J. J.; McMurry, T. J.; Lauffer, R. B. *Chem. Rev.* 1999, 99, 2293.

(2) Yoo, B.; Pagel, M. D. *Front. Biosci.* 2008, 13, 1733.

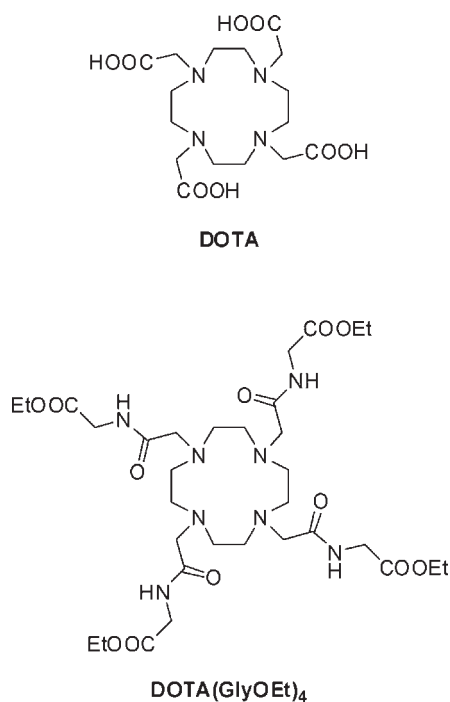
(3) Woods, M.; Zhang, S.; Sherry, A. D. *Curr. Med. Chem.: Immunol., Endocr. Metab. Agents* 2004, 4, 349.

(4) Merbach, A. E.; Toth, E. *The Chemistry of Contrast Agents in Medical Magnetic Resonance Imaging*; Wiley: Chichester, U.K., 2001.

(5) Major, J. L.; Meade, T. J. *Acc. Chem. Res.* 2009, 42, 893.

(6) Viswanathan, S.; Kovacs, Z.; Ratnakar, J.; Green, K. N.; Sherry, A. D. *Chem. Rev.* 2010, 110, 2960.

Chart 1



Ln(III) ions such as Eu(III), Tb(III), and Tm(III) induce large hyperfine shifts in most protons in a complex including any exchangeable NH and OH protons on the ligand arms and any bound water protons. The Ln(III)-bound water protons usually experience much larger hyperfine shifts than the ligand protons in all DOTA-like structures so these are particularly attractive for initiating CEST contrast. However, bound water lifetimes in these complexes can be too short for efficient CEST, so it is important to be able to manipulate water exchange using simple chemical principles. Eu(III) complexes with a variety of DOTA-tetraamides typically have sufficiently slow water exchange rates ( $\tau_m$  on the order of  $\mu\text{s}$ ) to satisfy the  $\Delta\omega > k_{\text{ex}}$  exchange requirement so these have been the most widely studied systems to date. In this study, we explored other types of ligand side-chains that can potentially offer a wider range of water exchange kinetics.

Lanthanide ions other than Eu(III) have also shown promise, but Eu(III) remains an area of piqued interest since these complexes typically display the longest bound water lifetimes.<sup>6</sup> Intrinsically, the bound water lifetime  $\tau_m$  is directly dependent on the electron deficiency at the lanthanide ion. Qualitatively, the greater the positive character remaining on the  $\text{Ln}^{3+}$ , the stronger the resulting  $\text{Ln}^{3+}-\text{OH}_2$  interaction will be. A negatively charged carboxylate group is electron rich and interacts more strongly with  $\text{Ln}^{3+}$  ions than an oxygen donor atom in the electron deficient amide. A comparison of resident water lifetime for the two  $\text{Gd}^{3+}$  complexes in Chart 1 clearly illustrates this effect:  $\text{GdDOTA}^-$  ( $\tau_m = 208 \text{ ns}$ ) vs  $\text{GdDOTA}(\text{GlyOEt})_4^{3+}$  ( $\tau_m = 190 \mu\text{s}$ ),<sup>8–10</sup> about

3 orders of magnitude different. Therefore, poor donors that leave the central lanthanide ion electron deficient are likely to produce slower water exchange systems (longer  $\tau_m$ ). There are many other factors that affect  $\tau_m$  including the coordination geometry of the complex (the SAP/TSAP ratio), steric constraints (bulkiness of side-chains), and hydrophobic/hydrophilic effects that alter second coordination sphere water molecules. In a recent paper, we have shown that Eu(III) complexes of DOTA tetraamide ligands with different amino acid extended side-chains produce remarkably different CEST effects.<sup>11</sup> Preliminary density functional theory (DFT) studies corroborated the relationship between weaker donors and longer  $\tau_m$ . Morrow and co-workers extended this theory to pendent alcohols, known to remain protonated upon binding to a lanthanide ion.<sup>12</sup>

$\beta$ -Diketones are common ligands for lanthanides and lanthanide  $\beta$ -diketonate complexes have found important practical applications ranging from NMR shift reagents to luminescent probes to components in optical devices.<sup>13–15</sup> In spite of this, a simple carbonyl oxygen as a donor atom for  $\text{Ln}^{3+}$  ions has not been widely used in polyamine-based ligands. Thus, as a part of our research to explore novel ligands for PARACEST agents, we set out to design, synthesize, and study cyclen (1,4,7,10-tetraazacyclododecane) derivatives with ketone pendant arms and their complexes with  $\text{Eu}^{3+}$ . The PARACEST properties of these complexes are the major focus of the work described in this paper.

## Experimental Section

**General Remarks.** All solvents and reagents were purchased from commercial sources and used as received unless otherwise stated.  $^1\text{H}$ ,  $^{13}\text{C}$  NMR, and CEST spectra were recorded on a VNMRs 400 MHz direct drive Varian console. MALDI mass spectra were acquired on an Applied Biosystems Voyager-6115 mass spectrometer. Metal analysis (ICP-MS, Galbraith) was obtained to calculate metal content in solution before using the metal complexes for CEST experiments.

**Fitting of CEST Spectra.** Numerical solutions to the Bloch equations modified for exchange were obtained by use of a nonlinear fitting algorithm in MATLAB. Experimental CEST spectra measured using multiple  $B_1$  powers were fit independently to obtain estimates of the water exchange rates.<sup>6,16</sup>

**DFT Studies.** Gas phase DFT calculations were performed using a hybrid functional (B3LYP) as implemented in Gaussian 03. For ligands 4–6 (see Chart 2) all atoms were optimized using the 6-311G(d,p) basis set, while 3-21G was used for the corresponding metal ion-based calculations. A frequency calculation of each showed that there were no imaginary frequencies, supporting

(7) Ward, K. M.; Aletras, A. H.; Balaban, R. S. *J. Magn. Reson.* **2000**, *143*, 79.

(8) Micskei, K.; Helm, L.; Brucher, E.; Merbach, A. E. *Inorg. Chem.* **1993**, *32*, 3844.

(9) Dunand, F. A.; Borel, A.; Helm, L. *Inorg. Chem. Commun.* **2002**, *5*, 811.

(10) Zhang, S.; Jiang, X.; Sherry, A. D. *Helv. Chim. Acta* **2005**, *88*, 923.

(11) Viswanathan, S.; Ratnakar, S. J.; Green, K. N.; Kovacs, Z.; De Leon-Rodriguez, L. M.; Sherry, A. D. *Angew. Chem., Int. Ed.* **2009**, *48*, 9330.

(12) Woods, M.; Woessner, D. E.; Zhao, P.; Pasha, A.; Yang, M.-Y.; Huang, C.-H.; Vasalitiy, O.; Morrow, J. R.; Sherry, A. D. *J. Am. Chem. Soc.* **2006**, *128*, 10155.

(13) Lee, J.; Brewer, M.; Berardini, M.; Brennan, J. G. *Inorg. Chem.* **1995**, *34*, 3215.

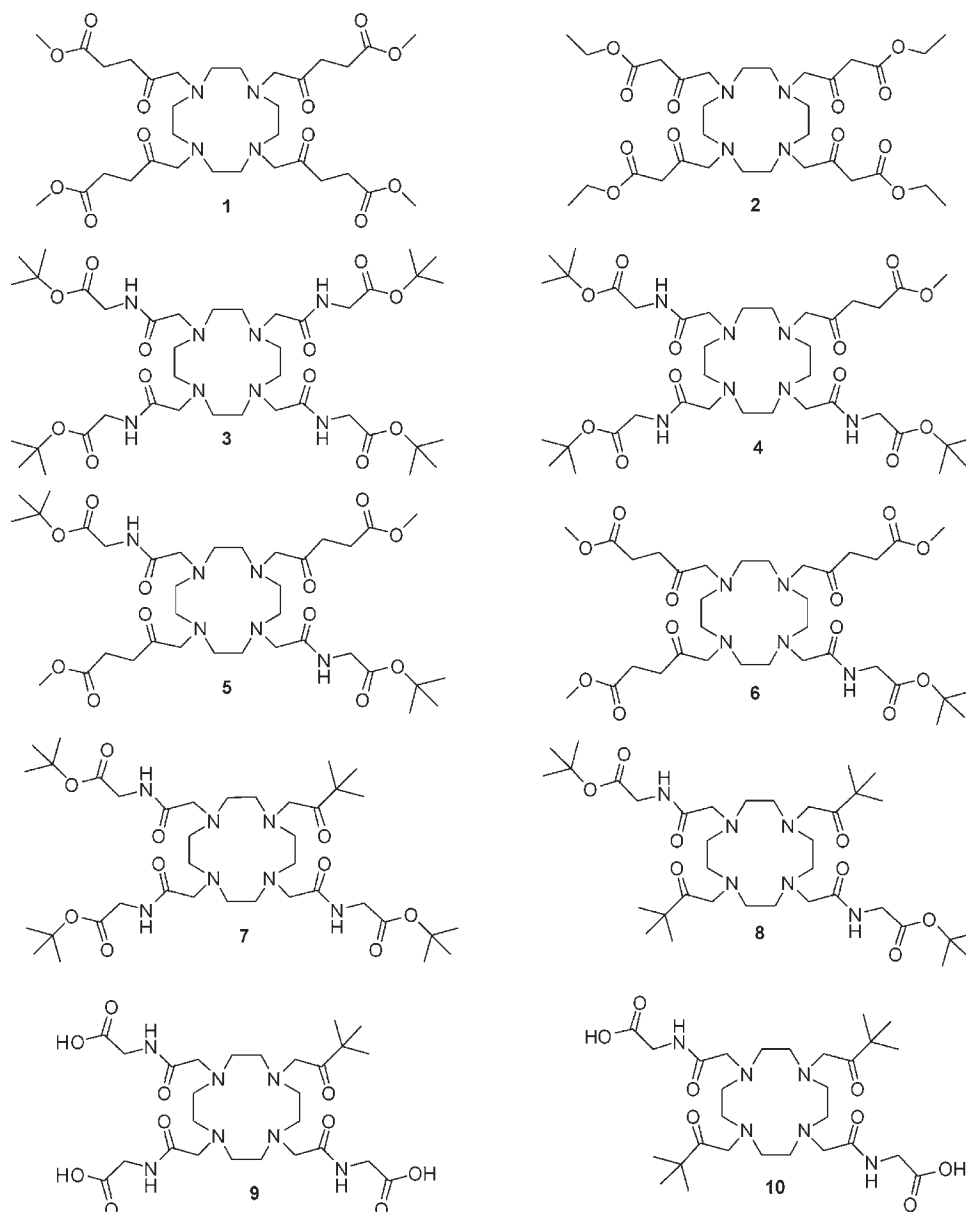
(14) Bunzli, J. C.; Choppin, G. R. *Lanthanide Probe in Life, Medical and Environmental Science*; Elsevier: Amsterdam, 1989.

(15) Huang, C. H. *Rare Earth Coordination Chemistry: Fundamentals and Applications*; Wiley: Singapore, 2010.

(16) Woessner, D. E.; Zhang, S.; Merritt, M. E.; Sherry, A. D. *Magn. Reson. Med.* **2005**, *53*, 790–799.

(17) Krogh-Jespersen, K.; Romanelli, M. D.; Melman, J. H.; Emge, T. J.; Brennan, J. G. *Inorg. Chem.* **2010**, *49*, 552.

Chart 2



a stable ground state. The .chk files of the optimized geometries were used to produce the Electrostatic Potential Plots and HOMO/LUMO orbital overlays in GaussView.<sup>17–21</sup>

(18) Frisch, M. J. T.; Trucks, G. W.; Schlegel, H. B.; Scuseria, G. E.; Robb, M. A.; Cheeseman, J. R.; Montgomery, Jr., J. A.; Vreven, T.; Kudin, K. N.; Burant, J. C.; Millam, J. M.; Iyengar, S. S.; Tomasi, J.; Barone, V.; Mennucci, B.; Cossi, M.; Scalmani, G.; Rega, N.; Petersson, G. A.; Nakatsuji, H.; Hada, M.; Ehara, M.; Toyota, K.; Fukuda, R.; Hasegawa, J.; Ishida, M.; Nakajima, T.; Honda, Y.; Kitao, O.; Nakai, H.; Klene, M.; Li, X.; Knox, J. E.; Hratchian, H. P.; Cross, J. B.; Bakken, V.; Adamo, C.; Jaramillo, J.; Gomperts, R.; Stratmann, R. E.; Yazyev, O.; Austin, A. J.; Cammi, R.; Pomelli, C.; Ochterski, J. W.; Ayala, P. Y.; Morokuma, K.; Voth, G. A.; Salvador, P.; Dannenberg, J. J.; Zakrzewski, V. G.; Dapprich, S.; Daniels, A. D.; Strain, M. C.; Farkas, O.; Malick, D. K.; Rabuck, A. D.; Raghavachari, K.; Foresman, J. B.; Ortiz, J. V.; Cui, Q.; Baboul, A. G.; Clifford, S.; Cioslowski, J.; Stefanov, B. B.; Liu, G.; Liashenko, A.; Piskorz, P.; Komaromi, I.; Martin, R. L.; Fox, D. J.; Keith, T.; Al-Laham, M. A.; Peng, C. Y.; Nanayakkara, A.; Challacombe, M.; Gill, P. M. W.; Johnson, B.; Chen, W.; Wong, M. W.; Gonzalez, C.; and Pople, J. A. *Gaussian 03*, revision D.01; Gaussian, Inc.: Wallingford, CT, 2004.

(19) Dickson, R. M.; Becke, A. D. *J. Chem. Phys.* **1993**, *99*, 3898.

**General Procedure for the Synthesis of the Eu<sup>3+</sup> Complexes.** A solution of europium triflate in acetonitrile (about 100 mg in 5 mL) was added to a solution of ligands **1** through **8** (up to 5% excess, to ensure that no free metal is present) in acetonitrile (5 mL). Each reaction was stirred at room temperature for 3 days before the solvent was removed under reduced pressure. Each residue was then dried under high vacuum to constant mass to afford the complex in quantitative yield. The complexes were judged over 95% pure by NMR and MS.

**Eu(1).** <sup>1</sup>H NMR (400 MHz, CD<sub>3</sub>CN) δ 13.2 (2H), 7.5(4H), 3.9(4H), 3.6(4H), 3.2 to -0.98(12H), -5.7(4H), -8.8(4H), -12.1(4H); *m/z* (ESI-MS, ESI<sup>+</sup>) 858.75 (100%, [M<sup>+</sup>OH<sub>2</sub>]<sup>3+</sup>), Calcd. 856.29.

**Eu(3).** <sup>1</sup>H NMR (400 MHz, CD<sub>3</sub>CN) δ 23.4(2H), 3.96(18H), 2.41(18H), 1.98(4H), 1.39 to -0.95(16H), -3.10(4H), -4.35(4H), -8.78(4H), -12.2(4H); MALDI+: *m/z* 1010.72 (100%) [M+H]<sup>+</sup>, Calcd. 1009.45.

**Eu(4).** <sup>1</sup>H NMR (400 MHz, CD<sub>3</sub>CN) δ 13.2(2H), 7.21(4H), 3.84(4H), 3.53(12H), 2.77(9H), 2.54(8H), 1.93 to -1.21(18H), -5.54(4H), 7.49(4H), 12.1(4H); *m/z* (ESMS, ESI<sup>+</sup>) 984.24 (100%, [M+OH<sub>2</sub>]<sup>3+</sup>), Calcd. 984.42.

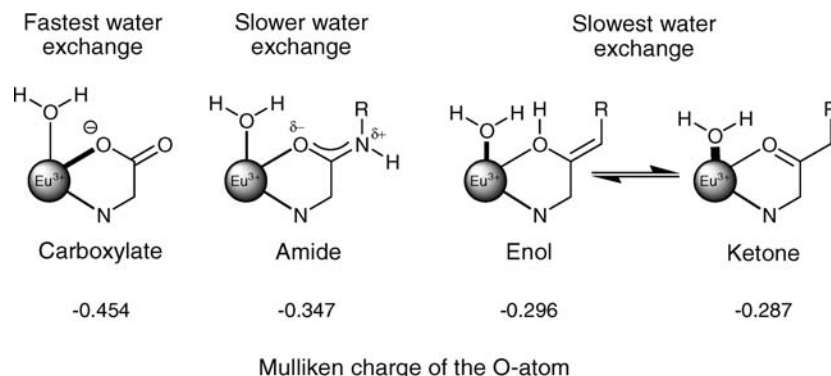


**Figure 1.** Expected resonance contributions in europium(III) chelate bonds in ligands containing a carboxylate oxygen, an amide oxygen, enol oxygen or a ketone oxygen donor, and the anticipated trends in the metal-bound water oxygen bond lengths and bound water residence lifetimes. The calculated Mulliken charges on the oxygen donor atom in each type of complex is also shown.

**Eu(5).**  $^1\text{H}$  NMR (400 MHz,  $\text{CD}_3\text{CN}$ )  $\delta$  35.7(2H), 21.1(4H), 19.9(4H), 15.69(4H), 14.73(4H), 9.40(12H), 7.21(12H), 6.45(9H), 3.45(4H), 3.24(4H), 2.47(4H), 2.37(6H), 1.78 to  $-1.45$ (24H),  $-2.96$ (4H),  $-3.37$ (4H),  $-5.62$ (4H),  $-9.19$ (4H),  $-13.02$ (4H),  $-15.40$ (4H),  $-16.69$ (4H),  $-17.33$ (4H);  $m/z$  (ESMS,  $\text{ESI}^+$ ) 941.14 (100%,  $[\text{M}+\text{OH}_2]^{3+}$ ), Calcd. 941.37.

**Eu(6).** A similar procedure to the synthesis of **Eu(1)** was followed.  $^1\text{H}$  NMR (400 MHz,  $\text{CD}_3\text{CN}$ )  $\delta$  13.4(2H), 7.27(4H), 6.12(4H), 4.79(4H), 4.11(4H), 3.77(6H), 3.63(8H), 3.48(9H), 3.23 to 1.08(8H),  $-1.2$ (4H);  $m/z$  (ESMS,  $\text{ESI}^+$ ) 897.482 (100%,  $[\text{M}+\text{OH}_2]^{3+}$ ) Calcd. 898.33.

**Eu(7).**  $^1\text{H}$  NMR (400 MHz,  $\text{CD}_3\text{CN}$ )  $\delta$  46.1(2H), 29.4(4H), 13.8(4H), 8.51(3H), 5.07(27H), 3.80(9H), 2.75 to 0.74(8H),  $-8.24$ (3H),  $-8.88$ (3H),  $-11.7$ (4H),  $-13.8$ (4H); MALDI $^+$ :  $m/z$  935.416 (100%),  $[\text{M}+\text{H}]^+$ , Calcd. 936.43.

**Eu(8).**  $^1\text{H}$  NMR (400 MHz,  $\text{CD}_3\text{CN}$ )  $\delta$  27.9(2H), 16.0(2H), 12.8(2H), 11.51(2H), 9.81(2H), 7.75(2H), 5.23(4H), 4.17(18H), 3.91(18H), 3.36 to  $-2.03$ (6H),  $-4.85$ (2H),  $-8.95$ (2H),  $-10.29$ (2H),  $-11.0$ (2H),  $-13.6$ (2H); MALDI $^+$ :  $m/z$  863.611 (100%),  $[\text{M}+\text{H}]^+$ , Calcd. 863.42.

**Eu(9).** A solution of  $\text{EuCl}_3$  (9.5 mg, 0.0367 mmol) was added to a solution of **9** (22 mg, 0.0367 mmol) in  $\text{H}_2\text{O}$  (5 mL total). The pH of the solution was maintained between 6 and 7 by the addition of NaOH solution for 24 h. At the end of this period, the pH was set to 8, and the sample was filtered and freeze-dried to afford the complex as a white solid.  $^1\text{H}$  NMR (400 MHz,  $\text{CD}_3\text{CN}$ )  $\delta$  28.3(2H), 21.65(2H), 18.93(2H), 6.15(2H), 4.62(2H), 4.27(2H), 4.05(3H), 3.97(3H), 3.81(3H), 3.64(2H), 3.47(2H), 3.32(2H), 3.21(2H), 2.82 to  $-5.07$  (8H),  $-5.54$ (2H),  $-7.71$ (2H),  $-8.06$ (2H),  $-11.0$ (2H),  $-12.9$ (2H); MALDI $^+$ :  $m/z$  768.08 (100%),  $[\text{M}+\text{H}]^+$ , Calcd 768.24.

**Eu(10).** A similar procedure to the synthesis of **Eu(9)** was followed.  $^1\text{H}$  NMR (400 MHz,  $\text{CD}_3\text{CN}$ )  $\delta$  25.8(2H), 17.98(2H), 14.02(2H), 7.95(6H), 4.63(6H), 3.68(6H), 3.25(2H), 3.13(2H), 2.96 to  $-0.641$ ,  $-1.48$ (2H),  $-8.53$ (2H),  $-12.5$ (2H); MALDI $^+$ :  $m/z$  750.944 (100%),  $[\text{M}+\text{H}]^+$ , Calcd 751.29.

## Results and Discussion

Our initial hypothesis postulated that cyclen derivatives with simple ketone pendant arms would donate considerably less electron density to a  $\text{Ln}^{3+}$  ion compared to amide donors, and this should result in a significant increase of the metal ion bound water lifetime (see Figure 1). Simple DFT calculation shows that the charge on a  $\text{C}=\text{O}$  oxygen decreases substan-

tially from a carboxylic acid to an amide to a ketone. Since it is now well documented that substituting an amide for a carboxylate donor atom in  $\text{Ln}$ -polyaminopolycarboxylate complexes substantially increases the bound water residence lifetime,<sup>6</sup> the DFT results summarized in Figure 1 predict that substitution of an even weaker ketone donor should produce complexes with even slower water exchange. The calculation does not allow us to predict the magnitude of the effect, however.

The series of chelates chosen to evaluate the variations in water exchange kinetics that might be possible in  $\text{Eu}^{3+}$ -based PARACEST agents are shown in Chart 2. The impact of ligand donor strength on water exchange kinetics were first explored in the ketone donor ligands **1** and **2**. We subsequently prepared mixed pendant arm ligands derived from DOTA-(gly tBu)<sub>4</sub> (ligand **3**) by sequentially replacing the extended glycinate side arms with levulonate (ligands **1**, **4**, **5**, and **6**) as well as the bulky pinacolone appendages (ligands **7**–**10**).

**Synthesis and Characterization of the Ligands and Their  $\text{Eu}^{3+}$  Complexes.** Synthesis of ligands **1**–**3** involved the tetraalkylation of cyclen with the appropriate bromo or chloro derivative of the ketone. Methyl 5-bromolevulinate, required for **1**, was prepared by the bromination of methyl levulinate using a slightly modified literature method.<sup>22,23</sup> Halide precursors used for the synthesis of **2** was commercially available. Ligand **3** first required acylation of the t-Bu protected glycinate arm followed by alkylation of cyclen. Standard alkylation protocols gave the desired ligands **1**–**3** in variable yields (37–75%). Attempted synthesis of the corresponding acid derivatives of **1** and **2** followed by acid hydrolysis resulted in extensive decomposition. Synthesis of the mixed side arm ligands, **4**–**10**, began with selectively protected cyclen derivatives prepared as previously reported (all synthetic details are provided in Supporting Information). All ligands were characterized by  $^1\text{H}$  and  $^{13}\text{C}$  NMR spectroscopy, HPLC, MALDI-Mass Spectrometry, and/or elemental analysis (Experimental Section).

The NMR spectrum of **2** provided evidence for keto–enol tautomerism of the side arms, a well-understood phenomenon for  $\beta$ -diketones. Prototropic rearrangements between the keto and the enol forms are acid–base catalyzed and occur readily in the presence of water. In general,

(20) Lee, C.; Yang, W.; Parr, R. G. *Phys. Rev. B: Condens. Matter Mater. Phys.* **1988**, *37*, 785.

(21) Dennington, R., II; Keith, T.; Millam, J. *GaussView*, V. G., Version 4.1; Semichem, Inc.: Shawnee Mission, KS, 2007.

(22) Sorg, A.; Siegel, K.; Brueckner, R. *Chem.—Eur. J.* **2005**, *11*, 1610.

(23) Zhang, Y.; Wu, L.; Li, F.; Li, B.-G. *Synth. Commun.* **2005**, *35*, 2729.

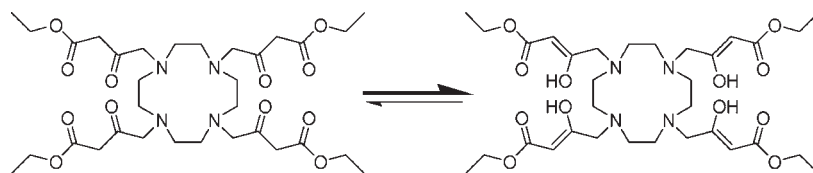
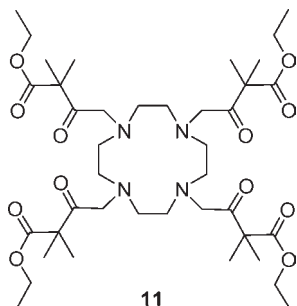
Scheme 1. Keto-Enol Tautomerism in Ligand **2**

Chart 3



simple ketones exist in the more stable keto form, but such compounds can exist in the enol form when stabilized by hydrogen bonding or steric factors.<sup>24</sup> A classic example is acetylacetone, a  $\beta$ -dicarbonyl compound in which the enol form is favored because of intramolecular hydrogen bonding. The  $^{13}\text{C}$  NMR of **2** showed that the  $\beta$ -dicarbonyl side chains exist predominantly in the enol form as evidenced by the upfield shift of the  $\alpha$ -carbonyl carbon to about 118 ppm (Scheme 1). In contrast, the absence of peaks around 120 ppm in the  $^{13}\text{C}$  NMR of ligand **1** (Supporting Information) suggests that this  $\gamma$ -dicarbonyl derivative exists primarily in the keto form, consistent with the fact that intramolecular stabilization of the enol form by H-bonding does not occur in  $\gamma$ -dicarbonyl compounds (Supporting Information, Figures S1 and S2).<sup>24</sup> Ligand **11**, shown in Chart 3, was designed to prevent keto–enol tautomerization via gem-dimethyl substitution on the carbon  $\alpha$  to the ketone carbonyl. As expected, enol species were not observed in the  $^{13}\text{C}$  spectrum of **11** (Supporting Information, Figure S3). NMR spectra of the remaining diketone ligands in Chart 2 (**4**, **5**, and **6**) showed no evidence for enol formation.

The  $\text{Eu}^{3+}$  complexes of **1–10** were prepared from the corresponding ligands by addition of either europium triflate in acetonitrile or europium chloride in water. The complexation reactions were run up to 3 days because of the slow formation kinetics of DOTA-like complexes.<sup>6</sup> The complexes were characterized by MALDI-mass spectrometry and  $^1\text{H}$  NMR. Although several routes were attempted, we were unable to obtain a  $\text{Eu}^{3+}$  complex of **11** likely because of the increased steric bulk of the gem-dimethyl groups. The  $^1\text{H}$  NMR spectra of **Eu(1)** and **Eu(2)** were recorded in  $\text{CD}_3\text{CN}$ . A notable feature of these spectra is that the observed  $\text{Eu}^{3+}$  induced  $^1\text{H}$  hyperfine shifts are significantly smaller than those of other  $\text{Eu}^{3+}$  DOTA-like complexes consistent with the anticipated weaker ligand field provided by the ketone donor groups. In both cases, a resonance observed near 15 ppm that disappeared upon addition of 10  $\mu\text{L}$  aliquots of  $\text{D}_2\text{O}$  to the sample was

tentatively assigned to a  $\text{Eu}^{3+}$ -bound water species. Similarly, resonances with similar exchange characteristics were seen in  $^1\text{H}$  NMR spectra of **Eu(4)** (46 ppm), **Eu(5)** (35 ppm), and **Eu(6)** (15 ppm). This trend is consistent with sequential substitution of amide side-arms with ketone side-chain donors (the  $\text{Eu}^{3+}$ -bound water resonance is near 50 ppm in most DOTA-tetraamide complexes). Closer inspection of the high resolution  $^1\text{H}$  NMR spectrum of **Eu(5)** showed that two coordination isomers were present in solution. 2D-EXSY spectroscopy of this complex showed interconverting species, consistent with square antiprism (SAP) and twisted square antiprism (TSAP) coordination isomers (Supporting Information, Figure S3).<sup>6,25</sup> Given that water exchange in TSAP isomers is generally about 2 orders of magnitude faster than in SAP isomers and, consequently, the  $\text{Eu}^{3+}$ -bound water resonance in the TSAP isomer is typically not detected by  $^1\text{H}$  NMR near room temperatures,<sup>6</sup> the exchangeable peaks observed here for **Eu(5)** are most logically assigned to the SAP isomer. Similarly, the exchangeable proton resonance seen in the NMR spectra of **Eu(1)**, **Eu(2)**, **Eu(4)** and **Eu(6)** likely also reflects SAP isomers in these complexes.

A proton exchangeable resonance (presumably  $\text{Eu}-\text{OH}_2$ ) was also observed in  $^1\text{H}$  NMR spectra of **Eu(7)**, **Eu(8)**, **Eu(9)**, and **Eu(10)** in  $\text{CD}_3\text{CN}$ . All resonances in the spectra of **Eu(7)** and **Eu(8)** were quite broad compared to the others, consistent with more dynamic, less rigid structures. Again, sequential replacement of amide side-arms with the more bulky *t*-butyl ketone arms resulted in an upfield shift in the  $\text{Eu}-\text{OH}_2$  resonances, consistent with earlier series. 2D-EXSY NMR of **Eu(8)** also indicated the presence of two interchanging isomers. Interestingly, the exchangeable  $\text{Eu}-\text{OH}_2$  resonances in **Eu(9)** and **Eu(10)** appear at 29 and 26 ppm, respectively, much less differentiated on the basis of chemical shift than the corresponding exchangeable  $\text{Eu}-\text{OH}_2$  resonances in the esters, **Eu(7)** and **Eu(8)**. This indicates that the ligand field created by the ligand side-arms is somewhat stronger in the ester versus the free acid complexes. Nonetheless, the general trend in  $\text{Eu}^{3+}$ -bound water chemical shifts with ketone substitution, albeit less pronounced, remains intact for this series of chelates as well. The observation that the  $\text{Eu}-\text{OH}_2$  proton resonance in **Eu(9)** appears further upfield than the corresponding  $\text{Eu}-\text{OH}_2$  proton resonances in other monosubstituted ketone derivatives (**Eu(4)** and **Eu(7)**) suggests that the greater negative charge in **Eu(9)** contributes to a weaker ligand field.

The relationship between the position of the  $\text{Eu}-\text{OH}_2$  resonance and the macrocycle  $\text{H}_4$  protons is another notable feature for this series of mixed donor ligands. For other  $\text{Eu}$ DOTA-tetraamide based systems, the  $\text{H}_4$

(24) Kemp, D. S.; Vellaccio, F. *Organic Chemistry*; Worth Publishers: New York, 1980.

(25) Vipond, J.; Woods, M.; Zhao, P.; Tircso, G.; Ren, J.; Bott, S. G.; Ogrin, D.; Kiefer, G. E.; Kovacs, Z.; Sherry, A. D. *Inorg. Chem.* **2007**, *46*, 2584.

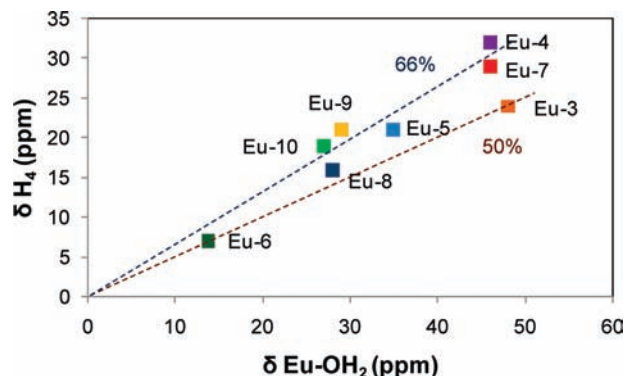


**Figure 2.** Comparison of chemical shifts of the Eu–OH<sub>2</sub> resonances vs the H<sub>4</sub> ligand proton resonances in each complex (measured in CD<sub>3</sub>CN). The two dashed lines correspond to 66% and 50% of the  $\delta \text{H}_4/\delta \text{Eu-OH}_2$  ratios, respectively.

resonance is consistently observed at a chemical shift about 50% that of the Eu–OH<sub>2</sub> resonance (determined by the geometry of the complex, see for example the data point for Eu(3) in Figure 2).<sup>6</sup> This relationship differs somewhat for the mixed ketone/amide systems (Figure 2). For chelates containing 3 amides and 1 ketone side-arms (Eu(4) and Eu(7)) the chemical shifts of H<sub>4</sub> protons are ~66% of the chemical shifts of the Eu–OH<sub>2</sub> resonances. For ligands containing 2 amide and 1 ketone side-arms (Eu(5) and Eu(8)), the chemical shift of the H<sub>4</sub> protons are ~60% of the chemical shift of the respective Eu–OH<sub>2</sub> resonances. The acid derivatives (Eu(9) and Eu(10)) follow a similar trend. The fact that this ratio changes with side arm substitution indicates that the geometry of the H<sub>4</sub> proton relative to the Eu-bound water protons differs somewhat in these complexes. If one assumes that the Eu–N bonds remain relatively constant among this series, then the larger hyperfine shift of H<sub>4</sub> relative to Eu–OH<sub>2</sub> can be explained entirely by lengthening of the Eu–water oxygen bond distance as amides are replaced by ketone side-chains. The absolute chemical shift of the H<sub>4</sub> protons can serve as a spectroscopic handle for the strength of the ligand field, with strong field ligands producing larger, downfield shifts. On the basis of the experimental observations then, substitution of an amide donor by a ketone donor clearly produces a weaker ligand field throughout this series.

**CEST Spectra and Metal Bound Water Residence Lifetimes.** CEST spectroscopy was used to determine the bound water lifetimes ( $\tau_m$ ) in each complex where a CEST exchange peak from the Eu<sup>3+</sup>-bound water molecule was observed (Supporting Information, Figures S4–S11). CEST spectra were collected either in a 1:1 mixture of water and acetonitrile or in pure water for the water-soluble acid derivatives, Eu(9) and Eu(10). The measured bound water lifetimes and the position of the Eu<sup>3+</sup>-bound water exchange peak are compiled in Table 1. The bound water lifetimes increased from 345 to 395 to 475  $\mu\text{s}$  along the series Eu(3), Eu(4), and Eu(5), supporting our hypothesis that an increase in the number of ketone donors does indeed slow water exchange (longer  $\tau_m$ ). A similar increase in  $\tau_m$  was observed from Eu(9) to Eu(10) but, interestingly, this was not observed for the corresponding esters, Eu(7) to Eu(8). The unexpectedly short  $\tau_m$  value of Eu(8) is because this complex has a lower SAP/TSAP ratio than Eu(7) (see later discussion).

**Table 1.** Chemical Shift of CEST Exchange Peaks and the Bound Water Lifetimes for Eu<sup>3+</sup> Complexes Examined in This Study

	$\delta \text{Eu-OH}_2$ (ppm)	$\tau_m$ ( $\mu\text{s}$ ) <sup>a</sup>	solvent
Eu(3)	48	345 ± 12	H <sub>2</sub> O/CH <sub>3</sub> CN <sup>b</sup>
Eu(4)	34	395	H <sub>2</sub> O/CH <sub>3</sub> CN <sup>b</sup>
Eu(5)	26	475	H <sub>2</sub> O/CH <sub>3</sub> CN <sup>b</sup>
Eu(7)	38	310 ± 5	H <sub>2</sub> O/CH <sub>3</sub> CN <sup>b</sup>
Eu(8)	26	185 ± 3	H <sub>2</sub> O/CH <sub>3</sub> CN <sup>b</sup>
Eu(9)	28	332 ± 5	H <sub>2</sub> O
Eu(10)	27	416 ± 12	H <sub>2</sub> O

<sup>a</sup> The  $\tau_m$  values were obtained by fitting the CEST data obtained at different B<sub>1</sub> values to the Bloch equations.<sup>16</sup> The  $\pm$  values represent the error in multiple fittings. <sup>b</sup> The ratio of H<sub>2</sub>O/CH<sub>3</sub>CN was 1:1.

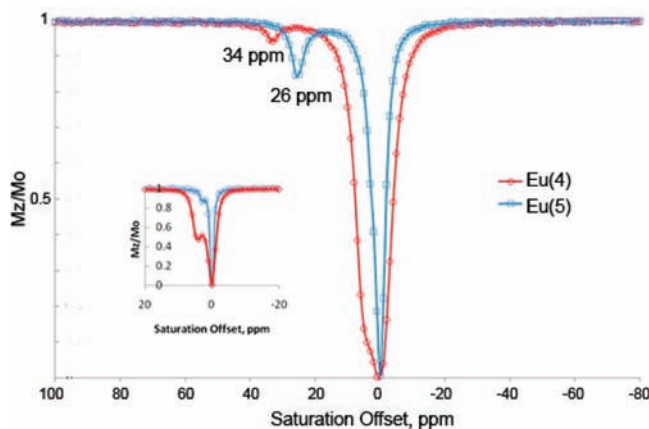


**Figure 3.** CEST spectra of Eu(4) (red) and Eu(5) (blue) recorded at 9.4 T and 298 K in CH<sub>3</sub>CN at B<sub>1</sub> = 10.8  $\mu\text{T}$  (459 Hz) and 10.0  $\mu\text{T}$  (426 Hz), respectively. (Inset: B<sub>1</sub> = 2.5  $\mu\text{T}$  for both spectra.)

For most complexes, a Eu<sup>3+</sup>-bound water exchange peak was observed at or near the same chemical shift as the one described above for the exchangeable bound water resonance as observed by high resolution <sup>1</sup>H NMR (spectra recorded in CD<sub>3</sub>CN). This suggests there may be some differences in the structures of some complexes in CD<sub>3</sub>CN as solvent versus 50:50 water/acetonitrile as solvent. For example, the high resolution <sup>1</sup>H spectra of Eu(4) and Eu(5) collected in nearly dry CD<sub>3</sub>CN show D<sub>2</sub>O exchangeable water peaks at 46 and 35 ppm, respectively, whereas the CEST spectra collected in 50:50 water/acetonitrile show exchangeable water peaks at 34 and 26 ppm, respectively (Figure 3). This suggests a chemical rearrangement occurs with the complex in water that results in a somewhat weaker ligand field experienced by the Eu<sup>3+</sup>, reflected by the ~25% smaller hyperfine shifts. Closer examination of the CEST spectra of Eu(4) and Eu(5), reveal that in addition to the Eu<sup>3+</sup>-bound water exchange peaks at 34 and 26 ppm, respectively, other exchanging peaks are present in these spectra near 5 and 3 ppm, respectively. Since these ligand side arms could in principle rearrange to the enol form in the presence of water (with the enol –OH acting as the ligand donor to the Eu<sup>3+</sup> ion), the peaks at 5 and 3 ppm could possibly reflect either Eu<sup>3+</sup>-bound –OH exchange peaks resulting from enol rearrangement or to a Eu<sup>3+</sup>-bound water molecule in the enol form of the complex. With either assignment, the observation that the Eu<sup>3+</sup>-bound water exchange peaks observed at 46 or 35 ppm (for Eu(4) and Eu(5),

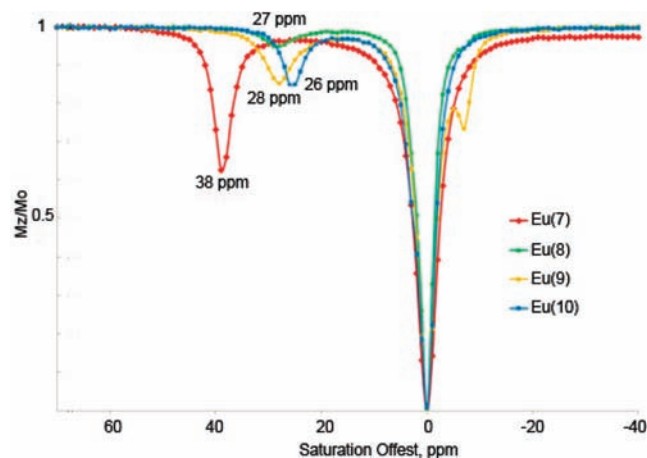


**Figure 4.** CEST spectra of Eu(7) (red, 17 mM), Eu(8) (green, 30 mM total, 12 mM SAP), Eu(9) (yellow, 18 mM), and Eu(10) (blue, 3.6 mM) recorded at 400 MHz and 298 K in H<sub>2</sub>O/CH<sub>3</sub>CN (1:1) for Eu(7) and Eu(8) and water for Eu(9) and Eu(10) using an applied  $B_1$  field of 10.4  $\mu$ T.

respectively) in neat acetonitrile shift to 34 and 26 ppm, respectively, in 50:50 water/acetonitrile indicates that the enol form ( $-\text{OH}$ ) provides a weaker ligand field than does the keto form. These putative  $-\text{OH}$  exchange peaks have similar chemical shifts as observed previously for  $-\text{OH}$  exchange peaks in  $\text{EuCNPHC}^{3+}$ , a complex having a single amide side-chain plus three hydroxyethyl side-chains (Supporting Information, Chart S1).<sup>12</sup> A previous report on this complex established that the hydroxyl groups remain protonated (and hence show exchange peaks in the CEST spectra) in predominantly acetonitrile solutions but disappear upon addition of excess water. Similarly, the CEST exchange peaks observed here for Eu(4) and Eu(5) disappear entirely when dissolved in 80:20 water/acetonitrile. This provides further evidence for the assignment of the small exchange peaks near 5 and 3 ppm in CEST spectra of Eu(4) and Eu(5) to exchanging enol  $-\text{OH}$  protons. The absence of enol  $-\text{OH}$  exchange peaks in CEST spectra of Eu(7–10) is also consistent with this assignment (Figure 4).

Interestingly, the CEST spectra of those complexes containing three or more ketone side-arms, Eu(1), Eu(2), and Eu(6) did not show a  $\text{Eu}^{3+}$ -bound water exchange peak in 50:50 H<sub>2</sub>O/CH<sub>3</sub>CN at room temperature. CEST spectra for these same complexes run in nearly dry CH<sub>3</sub>CN did show a small CEST exchange peak near 4 ppm, again consistent with either enol  $-\text{OH}$  exchange peaks or a weakly shifted  $\text{Eu}^{3+}$ -bound water exchange peak.

Figure 4 compares CEST spectra of Eu(7) and Eu(8) in H<sub>2</sub>O/CH<sub>3</sub>CN. The exchange peaks at 38 and 26 ppm, respectively, are easily assigned to  $\text{Eu}^{3+}$ -bound water exchange peaks based upon comparisons to their high resolution NMR spectra. As expected, ligand 8, with two ketone donor groups, produces a weaker ligand field for  $\text{Eu}^{3+}$  than does ligand 7 with only one ketone donor. This is manifested by the smaller  $\Delta\omega$  for the water exchange peak in Eu(8). However, the smaller  $\Delta\omega$  in this case does not translate to a longer bound water lifetime since Eu(7) displays slower water exchange ( $\tau_m = 310 \mu\text{s}$ ) than Eu(8) ( $\tau_m = 185 \mu\text{s}$ ) so other factors must come into play here.

One possibility is the presence of SAP versus TSAP isomers in these complexes. The <sup>1</sup>H NMR spectrum of Eu(7) shows that this complex exists in solution largely as the SAP isomer while the spectrum of Eu(8) shows two coordination isomers. 2D-EXSY spectroscopy of Eu(8) shows that these are interconverting SAP/TSAP species (data not shown) with the TSAP predominating (40% SAP, 60% TSAP). The CEST spectrum of Eu(8) also shows only a small  $\text{Eu}^{3+}$ -bound water exchange peak at 27 ppm, consistent with a small population of the SAP isomer in this sample. Given that water exchange in the predominant TSAP isomer is expected to be too fast to be observed by CEST in this species, its presence, however, will affect the measured residence water lifetime in samples consisting of lesser quantities of the SAP isomer.<sup>6</sup> This is the likely reason why  $\tau_m$  for Eu(8) is much smaller (185  $\mu\text{s}$ ) than what one might have anticipated based on its chemical structure.

The greater proportion of TSAP isomer found in Eu(8) likely reflects increased steric encumbrance around the  $\text{Eu}^{3+}$  ion imposed by the two bulky ketone side-arms placed in close proximity to the bulky *tert*-butyl groups on the glycinate arms. Removal of the *tert*-butyl ester groups had only a small impact on water exchange in complexes containing one ketone side arm (compare  $\tau_m$  in Eu(7) (310  $\mu\text{s}$ ) and Eu(9) 332  $\mu\text{s}$ ) but had a dramatic effect in complexes containing two ketone side-arms (compare  $\tau_m$  in Eu(8) (185  $\mu\text{s}$ ) and Eu(10) 416  $\mu\text{s}$ ). Unlike Eu(8), Eu(10) exists largely as a SAP isomer in solution (> 90%), so removal of the bulky *tert*-butyl ester groups has a rather dramatic effect on overall structure and on water exchange kinetics in this system. It is also interesting to note that the intensity of the  $\text{Eu}^{3+}$ -bound water exchange peaks in Eu(9) and Eu(10) were sensitive to changes in pH, showing optimal CEST intensities at pH = 6.4 and diminishing CEST with further increases in solution pH (Supporting Information, Figure S12). This may in part reflect the effects of pH on acid/base catalyzed keto–enol isomerization.

## Conclusions

A series of cyclen based ligands with ketone side arms were synthesized and PARACEST properties of the corresponding  $\text{Eu}^{3+}$  complexes examined. Ligands 1, 2, and 11 containing only ketone side arms established that keto–enol isomerization plays a role in structural makeup of this class of chelates and suggested that the ketone groups may prefer to bind with the metal ion in the enolate form. For  $\text{Eu}^{3+}$  complexes containing mixed donor (amide/ketone) side-chains, ligands 4–10, each amide to ketone substitution resulted in slower water exchange and smaller  $\Delta\omega$ , consistent with our hypothesis that weak field ligands will yield complexes with slower water exchange kinetics by placing more positive character on the central lanthanide ion. Other features including coordination geometry (Eu(8)) and steric hindrance (likely a component in Eu(7–10)) clearly influence water exchange and the resulting PARACEST properties. Although solvent compatibility will likely hinder the use of many of these systems to *in vitro* applications only, this work lays the foundation for the design of other, weak donor systems capable of producing slower water exchange.

**Acknowledgment.** Financial support from the National Institutes of Health (CA115531, RR02584, and EB004582)

and the Robert A. Welch Foundation (AT-584) is gratefully acknowledged. We gratefully acknowledge the Johann Deisenhofer laboratory for use of their computational equipment and programs.

**Supporting Information Available:** Synthetic procedures for the ligands,  $^{13}\text{C}$  NMR spectrum of ligands **1** and **2**, 2D-EXSY spectrum of Eu(**5**), CEST spectra of Eu(**3**)–Eu(**10**). This material is available free of charge via the Internet at <http://pubs.acs.org>.